Supplemental Material

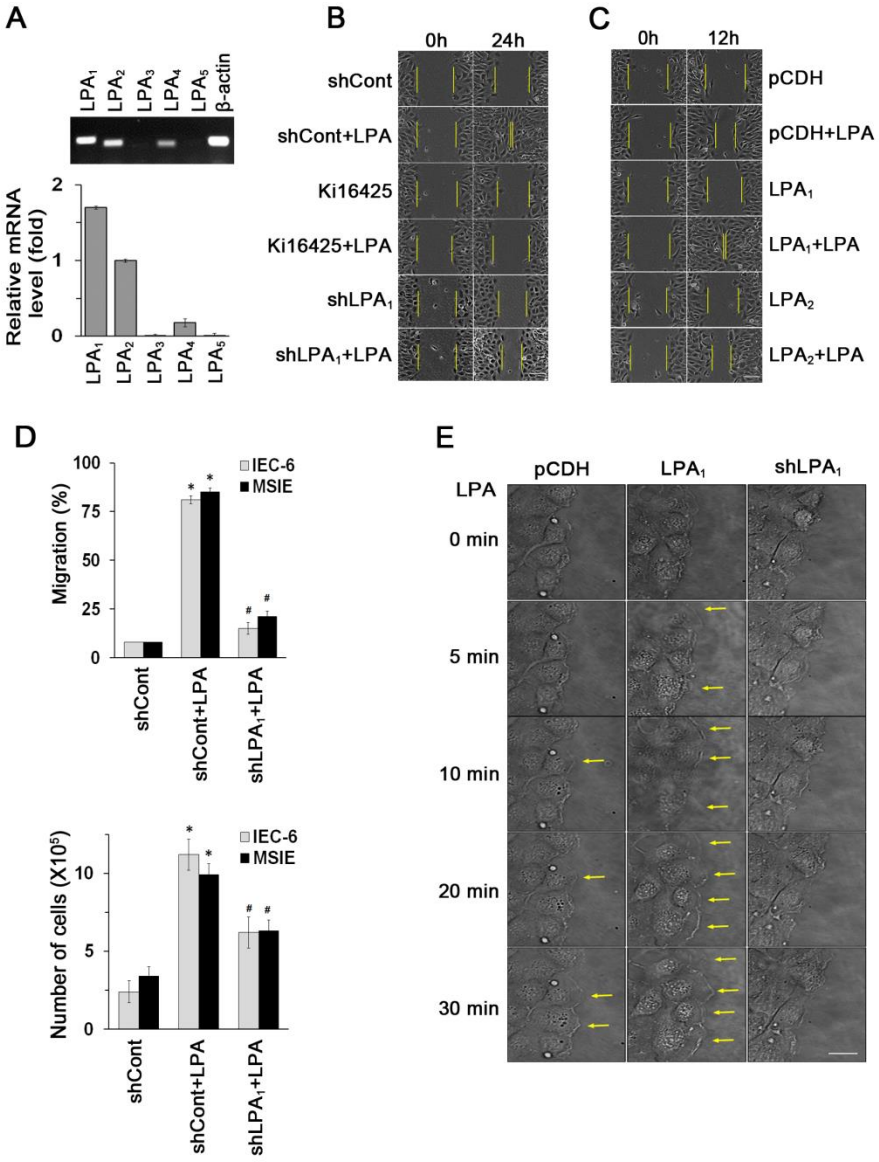

Fig. S1. LPA_1 mediates migration of IECs. (A) Expressions of LPA receptor in YAMC cells were determined by RT-PCR (top) and quantified by real-time RT-PCR (bottom). *n* = 3. **(B)** Migration of YAMC cells into the nude area at 24 h of 1 μM LPA treatment is shown. Cells were pretreated with 10 μM Ki16425 or transfected with $shLPA_1$ prior to LPA treatment. Scale bars, 20μm. *n* = 3. **(C)** Migration of YAMC cells overexpressing LPA_1 or LPA_2 was determined. Scale bars, 20μm. *n* = 3. **(D)** Migration of IEC-6 or MSIE cells during 24 h of LPA treatment is shown (top panel). Numbers of proliferating IEC-6 or MSIE cells at day 3 were determined (bottom panel). *, $P < 0.01$. #, $P < 0.01$. **(E)** The appearance of lamellipodial extrusion in YMAC cells transfected with pCDH, LPA_1, or $shLPA_1$ were captured by time-lapse video microscopy for 30 min. Representative sequential images are shown. Allows indicate lamellipoidia. *n* = 3. Scale bars, 20μm.

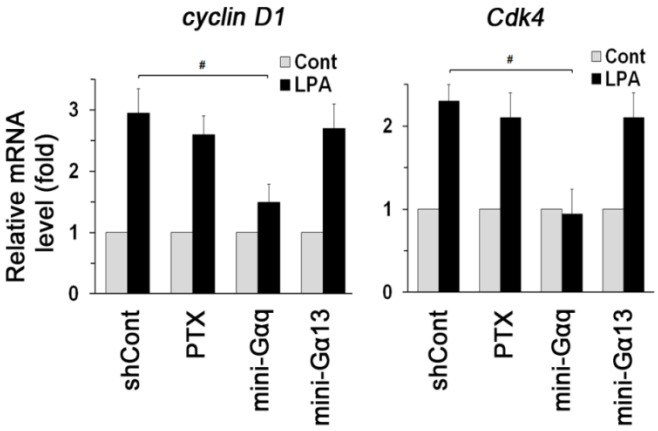

Fig. S2. Gαq regulates expression of cell cycle-related cyclin D1 and Cdk4. Expression levels of cyclin D1 and Cdk4 were determined by real-time RT-PCR. Cells are treated with PTX or transfected with minigene as indicated. $n = 3$. $^{\#}$, $P < 0.01$.

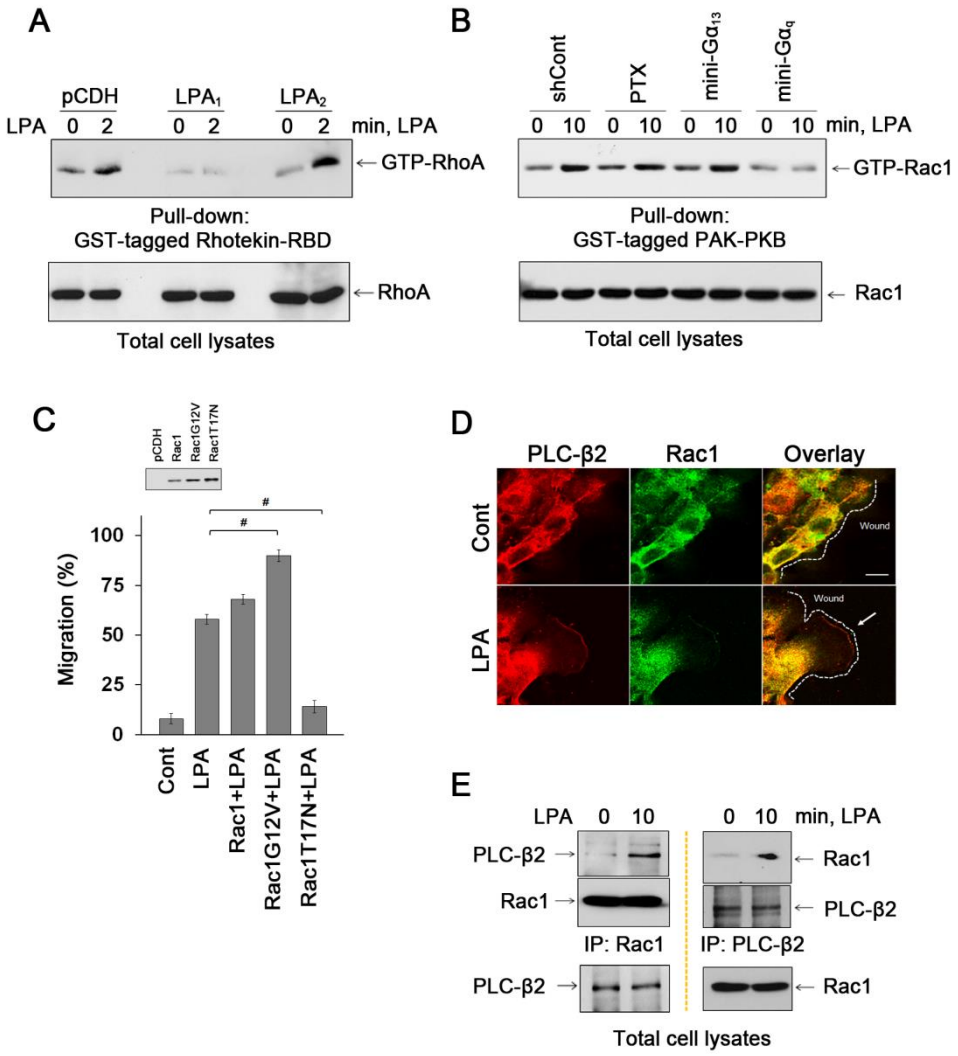

Fig. S3. Rac1 mediates LPA_1-induced cell migration. (A) Activation of RhoA in YAMC cells transfected with LPA_1 or LPA_2 was detected by GST-rhotekin RBD pull-down. Bottom panel shows RhoA in cell lysates. *n* = 3. **(B)** Rac1 activation was determined in YAMC cells pre-treated with PTX or transfected with minigene of Gαq or Gα13. Bottom panel shows Rac1 in cell lysates. *n* = 3**. (C)** Migration of YAMC cells transfected with Rac1, Rac1G12V, and Rac1T17N was determined. *n* = 3. $^{\#}$, P < 0.01 The inset shows expression of exogenous Rac1, Rac1G12V, and Rac1T17N in YAMC cells. **(D)** Co-localization of PLC-β2 (red) and Rac1 (green) at lamellipodia determined by immunofluorescence confocal microscopy. Arrow indicates lamellipodia. Outlined dash indicates leading edge. Scale bars, 20μm. **(E)** Cell lysates were immunoprecipitated with anti-Rac1 or anti-PLC-β2 antibody. Co-immunoprecipitated PLC-β2 (left) and Rac1 (right) was detected by Western blot. The bottom panels show expression of PLC-β2 and Rac1. *n* = 3.

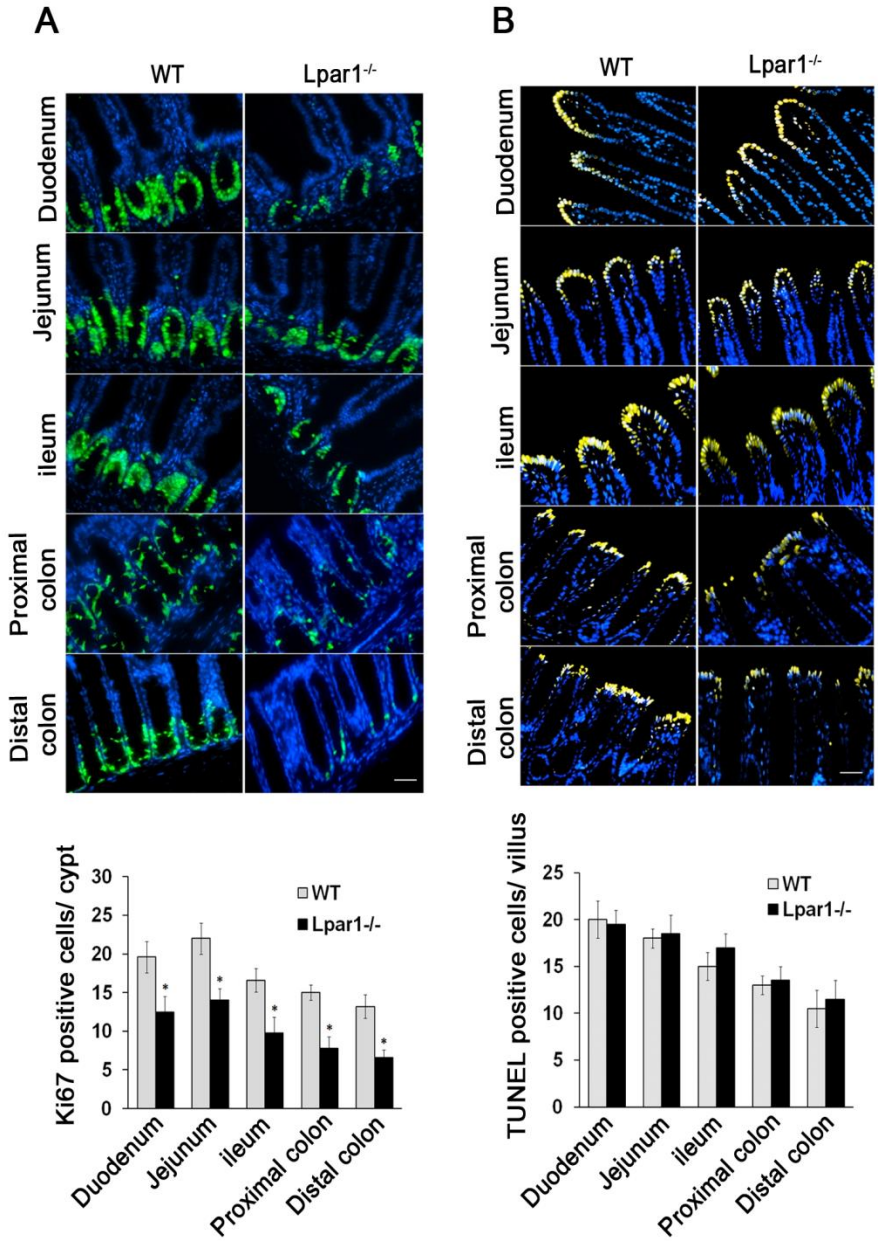

Fig. S4. **Cell proliferation but not apoptosis is altered in *Lpar1*$^{-/-}$ mice. (A)** Proliferating IECs in WT and *Lpar1*$^{-/-}$ intestine were immunolabeled using anti-Ki67 antibody (green). *n* = 6. DAPI was used for nuclear counterstaining (blue). Scale bars, 50μm. *, P < 0.01 versus WT. Numbers of proliferation cells are quantified in the graph below, **(B)** The apoptotic cells (yellow) in paraffin embedded sections were detected by TUNEL assay using an apoptosis detection kit according to manufacturer's instructions (R&D Systems). Quantification of TUNEL-positive cells is shown below.

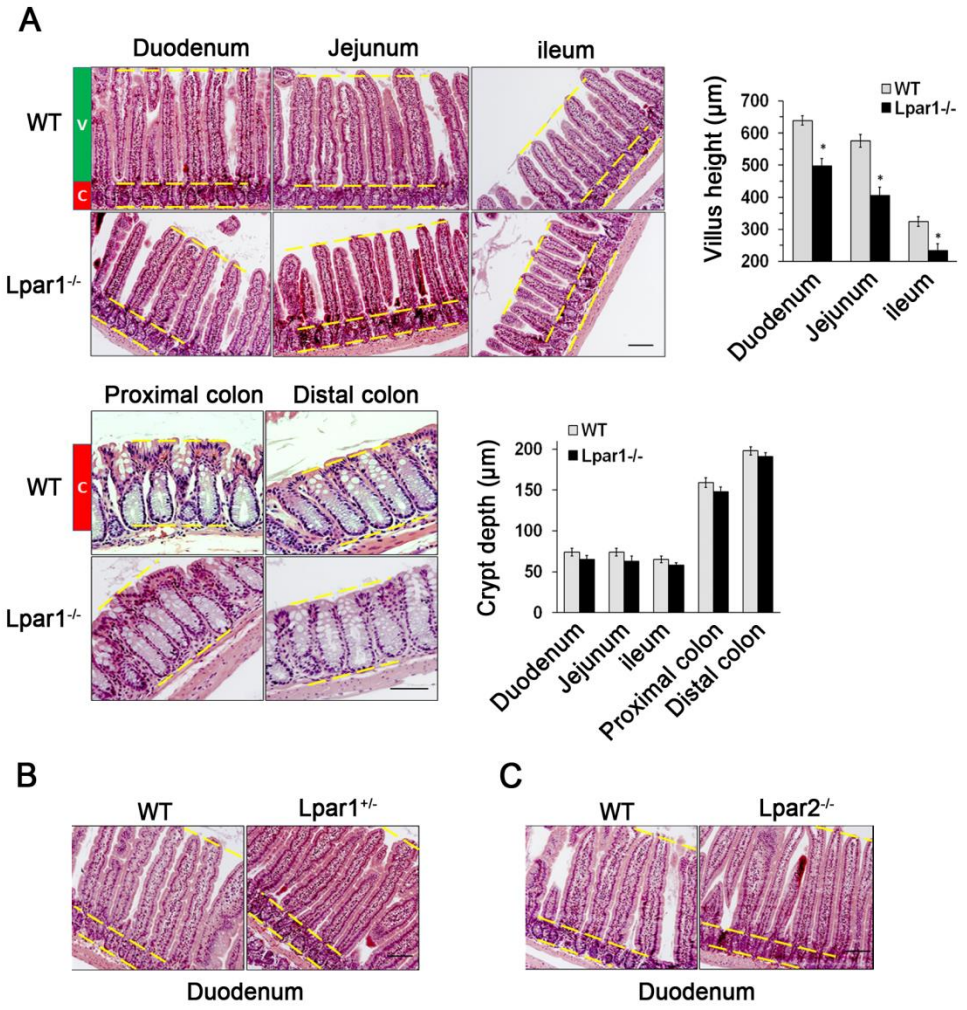

Fig. S5. ***Lpar1*$^{-/-}$ mice display shortened villi. (A)** Representative intestinal and colonic tissues stained with H&E are shown. Dash lines mark villus (v) and crypt (c). Graphs show quantification of villous height and crypt depth. *n* = 6 per group. Scale bars, 100μm. *****, P < 0.01 versus WT. The intestinal epithelial structures are not altered in *Lpar1*$^{+/-}$ **(B)** and *Lpar2*$^{-/-}$ **(C)** mice. *n* = 6. Scale bars, 100μm.